JOURNAL OF CATALYSIS 151, 241–252 (1995)

Vanadia/Titania Catalysts for Selective Catalytic Reduction of Nitric Oxide by Ammonia

II. Studies of Active Sites and Formulation of Catalytic Cycles[1]

N.-Y. Topsøe,[2] J. A. Dumesic,[3] and H. Topsøe
Haldor Topsøe Research Laboratories, DK-2800 Lyngby, Denmark

Received June 13, 1994; revised September 21, 1994

The reaction mechanism and catalytic cycle for the selective catalytic reduction of nitric oxide by ammonia over vanadia/titania catalysts has been elucidated by *in situ* on-line FTIR studies under steady-state conditions. Under all reaction conditions, a large concentration of ammonia is adsorbed on both Lewis and Brønsted acid sites, whereas no significant amounts of adsorbed NO are adsorbed. The catalytic activity is found to be related to the ammonia adsorbed on the Brønsted acid sites associated with V^{5+}–OH. Surface V=O groups are involved in activation of the adsorbed ammonia and are also found to play an important role in the catalytic cycle. The activation involves a transfer or a partial transfer of a hydrogen and reduced V–OH groups are produced. The V^{5+}=O surface species are regenerated by oxidation. The results, therefore, show that the catalytic cycle consists of both acid–base and redox reactions. The ammonia adsorption is observed to be a fast equilibrated step under all the conditions studied but the other catalytically significant steps may shift depending on the reaction conditions. At high O_2 partial pressures, the rate is mainly determined by the concentration of Brønsted acid sites and the NO partial pressure, whereas at low O_2 partial pressures, surface reoxidation is slow and the rate becomes dependent on the concentration of V^{5+}=O groups. © 1995 Academic Press, Inc.

INTRODUCTION

Many different types of reaction mechanisms have been proposed in the literature for the selective catalytic reduction of nitric oxide by ammonia over vanadia–titania catalysts in the presence of oxygen (1). These mechanisms range from Eley–Rideal-type processes not involving strongly adsorbed NO species to processes where NO is adsorbed in some manner. Adsorbed NO has also been suggested to play a role in a number of quite different proposals for the mechanism. Odriozola *et al.* (2) considered V_2O_5/TiO_2 as a bifunctional catalyst and suggested a Langmuir–Hinshelwood reaction between adsorbed NO on TiO_2 and adsorbed NH_3 on V^{5+}. Went *et al.* (3) proposed a mechanism involving a reaction between adsorbed NH_3 on Lewis acid sites and adsorbed NO on some other unspecified sites. Such proposals are apparently not in agreement with the failure to observe significant amounts of adsorbed NO under reaction conditions (4–6). Our previous TPD studies (7) have also shown that the adsorption of NO is weak. Takagi *et al.* (8, 9) proposed a Langmuir–Hinshelwood-type reaction between adsorbed NO_2 and adsorbed NH_4^+. However, such a mechanism does not appear likely since later studies of Inomata *et al.* (10) did not observe oxidation of NO to NO_2 by O_2 in a flow of dilute gases (1000 ppm NO in 1% O_2) which resembles that encountered under industrial conditions. Furthermore, recent direct *in situ* studies of such catalysts, Topsøe and Topsøe (4) did not detect NO_2 on the catalyst surface under typical SCR conditions.

Eley–Rideal-type reaction mechanisms between adsorbed NH_4^+ and gas-phase NO have been proposed by Inomata and co-workers (10, 11) and by Gasior *et al.* (6) Bosch *et al.* (12) proposed a redox mechanism where V^{5+} is first reduced by NH_3 and is subsequently reoxidized by NO via an Eley–Rideal-type reaction, producing nitrogen. This mechanism has also been favored by Janssen *et al.* (13). More recently, Ramis *et al.* (14) also proposed a redox mechanism in which the reaction takes place between a strongly adsorbed form of ammonia and gaseous or weakly bonded NO. However, different adsorption sites and mechanistic details were suggested in the above studies. Inomata and co-workers (10, 11) proposed that NH_3 adsorption occurs on dual sites involving V–OH and an adjacent V=O which assists in the activation of NH_3. They found that the rate of NH_3–NO reaction is proportional to the amount of V=O. Later studies (15–17),

---

[1] Presented at the ACS Spring Meeting, San Diego, March 1994.

[2] To whom correspondence should be addressed.

[3] Permanent address: Department of Chemical Engineering, University of Wisconsin, Madison, WI 53706.

0021-9517/95 $6.00

however, showed lack of correlation between V^{5+}=O and SCR activity. Gasior et al. (6) proposed V–OH to be the active site. This suggestion has since been supported by several investigators (15–17). The interaction of ammonia and V–OH was confirmed by Topsøe (17), who, in fact, observed a direct correlation between the concentration of V–OH groups and the Brønsted acidity.

Recently, Dumesic *et al.* (18) evaluated different mechanisms in a kinetic analysis of the deNO$_x$ reaction. It was shown that a simple two-step Eley–Rideal mechanism involving reaction between adsorbed NH_3 and gaseous (or weakly adsorbed) NO is not consistent with all data. Rather, these authors proposed a three-step mechanism (18) consisting of equilibrated ammonia adsorption, followed by an activation step of the adsorbed ammonia and a subsequent reaction between the activated ammonia species and NO. It was shown that it was not possible to distinguish kinetically whether this last step was a true Eley–Rideal step involving reaction with gaseous NO or a reaction with weakly adsorbed NO. The three-step mechanism was able to quantitatively describe the NO conversion data under industrial-type conditions for the vanadia/titania catalysts. Furthermore, it gave at the same time a very good description of the ammonia slip behavior which was found to be much more difficult to describe than the conversion of NO$_x$. Although this mechanism was also shown to be consistent with several independent observations (18), it can still be regarded as semi-empirical in nature due to the fact that detailed information on the surface chemistry was not available at the time.

In view of this situation, we have carried out a series of investigations of vanadia/titania catalyst systems in which *in situ* FTIR spectroscopic studies of the surface chemistry are combined with steady-state or transient on-line activity measurements. The preceding paper (19) dealt with the transient studies. The objective of the present paper is to formulate a catalytic cycle based on these *in situ* on-line results and the information obtained from the transient studies. A brief account of some of the findings has been given recently (20).

EXPERIMENTAL

The series of vanadia/titania catalysts and the titania support investigated in this study are the same as those used in the preceding paper (19). This previous paper also described the preparation of the samples and the methods for FTIR measurements.

Prior to reaction studies, each sample (100 mg) was oxidized in a flow of 8% O_2/Ar at 673 K for 14 h. A reaction gas mixture, prepared in an attached gas handling manifold, with the desired concentrations of NH_3, NO, and O_2, was passed over the sample at 1 atmosphere and the desired temperature. Unless otherwise specified, the flow rate was 150 N ml/min.

The catalyst surface was monitored *in situ* during selective catalytic reduction (SCR) reaction conditions by a Digilab FTS80 FTIR spectrometer equipped with a liquid N_2 cooled Mercury–Cadmium–Telluride (MCT) detector. A Balzers QMG420 mass spectrometer described earlier (4) was used on-line for the simultaneous measurement of the concentration of reactants and products. The mass spectrometer data were quantitatively analyzed using the fragmentation patterns determined experimentally from calibration gases.

The isotopic tracer study was carried out by dosing 3 Torr of ^{15}NO (>99% enriched from Prochem) onto the vanadia/titania catalyst with preadsorbed $^{14}NH_3$ after removal of excess gaseous ammonia.

RESULTS

Figures 1a–1d show *in situ* IR spectra in flowing O_2/Ar at 525 K of oxidized TiO_2, 0.6, 2, and 6 wt% V_2O_5/TiO_2, respectively. Figure 1e–1h show the corresponding spectra at the same temperature during SCR reaction using as feed a mixture of 500 ppm NO, 500 ppm NH_3, and 8% O_2 (the balance being Ar). These concentrations of NO, NH_3, and O_2 are similar to those encountered during industrial SCR operation. The same ammonia absorption bands are present in the spectra of Figs. 1e–1h as in spectra obtained after ammonia adsorption at room temperature (17), i.e., bands due to NH_4^+ (3019, 2808, 1670, and 1430 cm^{-1}) and coordinated NH_3 (3364, 3334, 3256, 3170, 1605, and 1220 cm^{-1}). However, a significantly lower intensity is seen for these bands on all samples at reaction conditions. Thus, the surface is apparently not completely saturated by ammonia under these conditions. The highest concentration of NH_4^+ on the surface is seen for the 6% vanadia/titania catalyst, followed by the catalysts with 2 and 0.6 wt% vanadia. The catalyst with the lowest vanadia loading has only a very small amount of NH_4^+ on the surface. No significant amount of NH_4^+ species can be detected at reaction conditions on the titania support, which shows mainly NH_3 coordinatively bonded to the surface.

In contrast to NH_3 adsorption studies at room temperature where essentially all OH groups are removed by interaction with NH_3 (17), the presence of bands between 3600 and 3750 cm^{-1} for all samples under reaction conditions indicates that some free OH groups are present during reaction. The V–OH groups are the sites that react with NH_3 to form NH_4^+ species (17). Thus, the presence of free V–OH bands under reaction conditions with an intensity slightly lower than for the oxidized samples reflects a partial surface coverage of NH_3. Table 1 shows the fractional ammonia coverages, θ, during reaction esti-

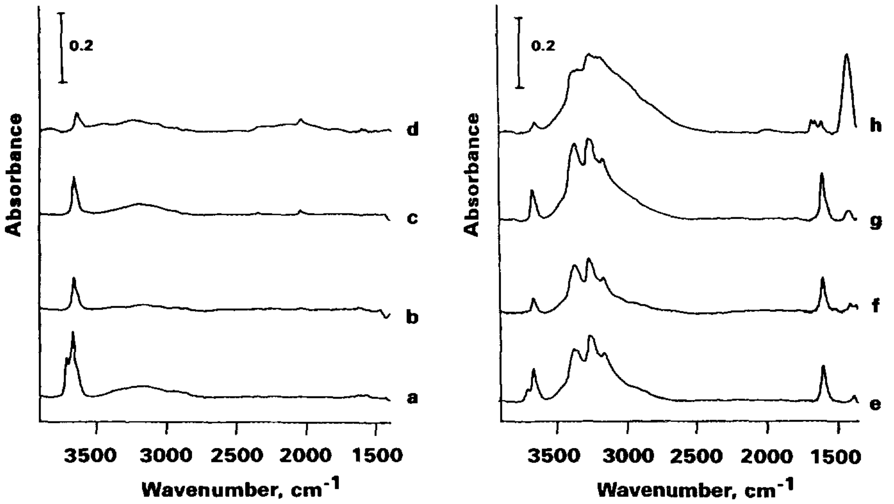

FIG. 1. (a–d) *In situ* IR spectra of the oxidized TiO_2, 0.6, 2, and 6% V_2O_5/TiO_2, at 525 K, respectively; (e–h) the corresponding spectra of these samples under SCR conditions at the same temperature.

mated from analyzing the NH_4^+ bands (θ_{BA}), the coordinated NH_3 bands (θ_{LA}), and the concentration of free OH groups (θ_{OH}), where BA denotes Brønsted acid and LA denotes Lewis acid. The first two values are relative to the band intensities at saturation ammonia coverage at room temperature, while the value of OH species is the difference in band intensity relative to the band intensity for the sample in O_2 at the reaction temperature. Table 1 shows that the BA/LA ratio increases with increasing vanadia loading in accordance with earlier results (19). The ammonia coverages, especially θ_{BA}, decrease with increasing temperature. This behavior is in accordance with the general observation of lower heats of ammonia adsorption on BA compared to LA sites (7).

It should be mentioned that the NH_3 saturation coverage in the absence of SCR reaction cannot be obtained at the high temperatures by exposure to pure NH_3 since NH_3 at these temperatures reduces the catalyst (see below). The NH_3 coverages were therefore measured in $NH_3 + O_2$ mixtures (Table 1). The NH_4^+ surface coverage, θ_{BA}, is similar to that observed during the reaction experiments, suggesting that NH_3 adsorption process is

TABLE 1

Ammonia Coverage on the Different Sites on the Catalyst Surface

	$NH_3 + NO + O_2$ (525 K)			$NH_3 + NO + O_2$ (625 K)			$NH_3 + O_2$ (525 K)		
Sample	θ_{OH}	θ_{BA}	θ_{LA}	θ_{OH}	θ_{BA}	θ_{LA}	θ_{OH}	θ_{BA}	θ_{LA}
TiO_2	.5	0	.5	.5	0	.3	—	—	—
0.6% V_2O_5/TiO_2	.6	0	.5	.5	0	.4	—	—	—
2% V_2O_5/TiO_2	.2	.2	.6	—	.1	.3	—	—	—
6% V_2O_5/TiO_2	.3	.3	~.2	.2	.1	.1	.7	.3	~.3

Note. The ammonia coverage on OH groups, θ_{OH}, during reaction at temperature T is calculated from

$$\theta_{OH} = \frac{A_{OH,ox} - A_{OH,rx}}{A_{OH,ox}},$$

where $A_{OH,ox}$ and $A_{OH,rx}$ refer to band intensities at temperature T in O_2 and under reaction conditions, respectively.

The ammonia coverage on Brønsted (Lewis) acid sites, ($\theta_{BA}(\theta_{LA})$), during reaction at temperature T is determined from the saturation coverage at room temperature ($A_{BA,rt}$ ($A_{LA,rt}$)) according to:

$$\theta_{BA(LA)} = \frac{A_{BA(LA),rx}}{A_{BA(LA),rt}}.$$

equilibrated. It is interesting that the ammonia coverage estimated from analyzing the decrease in intensity of the OH groups (θ_{OH}) appears to be lower under SCR reaction conditions than in the NH_3 + O_2 mixture. In view of the similarity in the coverages determined directly from the intensities of the NH_4^+ bank (θ_{BA}) in both cases, it does not appear that the ammonia coverage is very different under these two sets of conditions. Rather, the low value calculated from the OH groups may indicate the formation of new OH groups during reaction as also observed in the transient experiments (19).

Detailed analyses of the OH and the V=O groups on the different samples are shown in Figs. 2 and 3. Figure 2 shows the OH stretching region of the titania support, the 0.6, 2, and 6% vanadia/titania catalysts, both in flowing O_2 (Figs. 2a–2d) and under SCR reaction conditions at 525 K (Figs. 2e–2h). Previous studies of the OH region at room temperature (19) for the 0.6 and 2% samples showed that the OH band envelope consists of some overlap of the Ti–OH groups of the support and V–OH bands, whereas the 6% sample shows mainly a V–OH band at 3642 cm^{-1}. It is seen for all the samples that the intensities of the OH bands are generally lower in the reaction gas mixture than in O_2. As discussed above, this behavior is due to the partial coverage of V–OH groups by ammonia. A comparison of the OH band positions under SCR conditions and in O_2 shows a slight upward shift for the vanadia/titania catalysts but no such shift for TiO_2. The upward frequency shifts observed for the vanadia-containing catalysts indicate that the V cation bonded to OH has undergone reduction or that some new OH groups bonded to more reduced V species have formed. The latter explanation is favored since, as discussed above, the band intensities of free V–OH groups under SCR reaction conditions are higher than those determined with the sample in NH_3 + O_2. Thus, the spectra under SCR conditions consist of free V–OH groups similar to those originally present on the catalyst surface and additional V–OH groups associated with reduced V centers formed during the reaction. The observation that only intensity changes and no frequency shifts are seen for the titania support under SCR conditions indicates that the nature of the Ti–OH group remains unchanged during exposure to the reaction mixture. Therefore, these results confirm that the reactions operative over vanadia/titania catalysts are related to the presence of the vanadia.

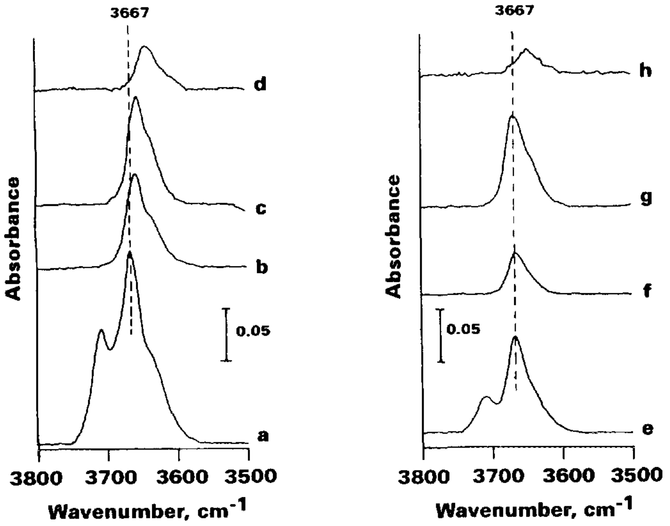

FIG. 2. (a–d) *In situ* IR spectra of the OH region of the oxidized TiO_2, 0.6, 6, 2, and 6% V_2O_5/TiO_2 at 525 K, respectively; (e–h) the corresponding OH spectra of these samples under SCR conditions at similar temperature.

Figures 3a–3c show the V=O overtone band regions at 525 K after oxidation of the 0.6, 2, and 6% vanadia/titania catalysts, respectively. The corresponding spectra obtained *in situ* under SCR reaction conditions are shown in Figs. 3d–3f. For a clearer analysis of the differences caused by the reaction, Figs. 3g–3i show the difference spectra, where the initial spectra obtained in O_2/Ar have been subtracted from those in the reaction mixture. Thus, negative bands indicate species that have been removed by reaction. In the spectra of the oxidized catalysts, the band maximum is quite constant at 2040 cm^{-1} with a shoulder near 2020 cm^{-1}, and the band intensity increases with increasing vanadia loading. Upon switching to the SCR reaction mixture, this band at 2040 cm^{-1} is nearly completely eliminated. The contribution of the shoulder band becomes apparent at 2025 cm^{-1} (Figs. 3d–3f) and is only partially removed in the reaction mixture (Figs. 3g–3i). Besides the removal of these bands, a broad band is formed near 1970 cm^{-1} which is most prominent in the high loading sample. The band at 2040 cm^{-1} has been assigned by several authors (17, 21–26) as the overtone band of the terminal V=O of monomeric vanadyls. The results in our previous paper (19) are consistent with this interpretation. The simultaneous disappearance of the 2040 cm^{-1} band and appearance of the 1970 cm^{-1} band may reflect a weakened vanadyl bond associated with a more reduced V center resulting from a perturbation by surface ammonia (19, 23, 25, 27).

To relate the various surface species and spectral changes observed with catalyst performance, on-line activity measurements were carried out simultaneously with the *in situ* FTIR spectroscopic investigations by monitoring mass spectrometrically the inlet and outlet gas compositions. The results from such combined measurements on TiO_2, 0.6, 2, and 6% vanadia/titania are summarized in Fig. 4. Since a detailed kinetic analysis is not necessary for the discussion of the observed trends, the data are simply represented in terms of the conver-

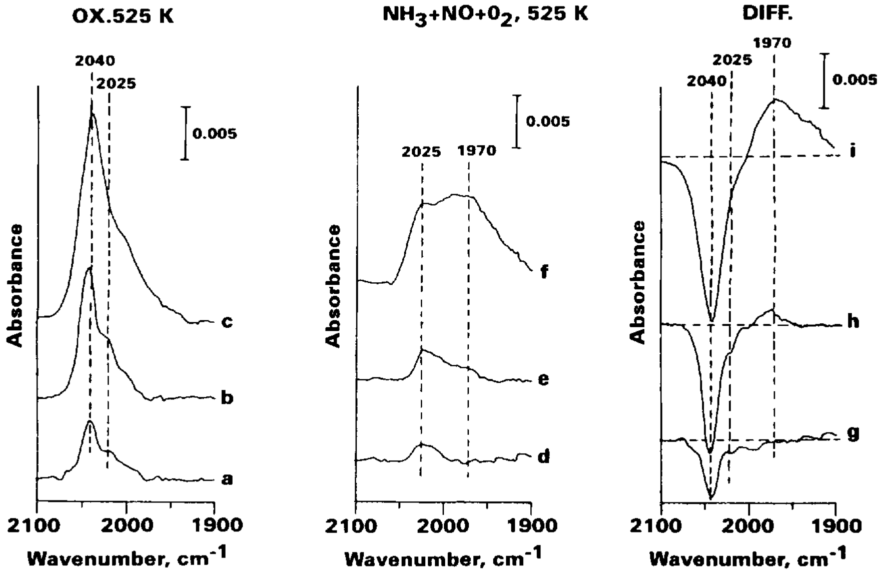

FIG. 3. (a–c) *In situ* IR spectra at 525 K of the V=O overtone band region of the 0.6, 2, and 6% V_2O_5/TiO_2 after oxidation, respectively; (d–f) the corresponding spectra of these samples under SCR condition at 525 K (gas phase NO subtracted); (g–i) the difference spectra where the background spectra prior to reaction have been subtracted from those under reaction.

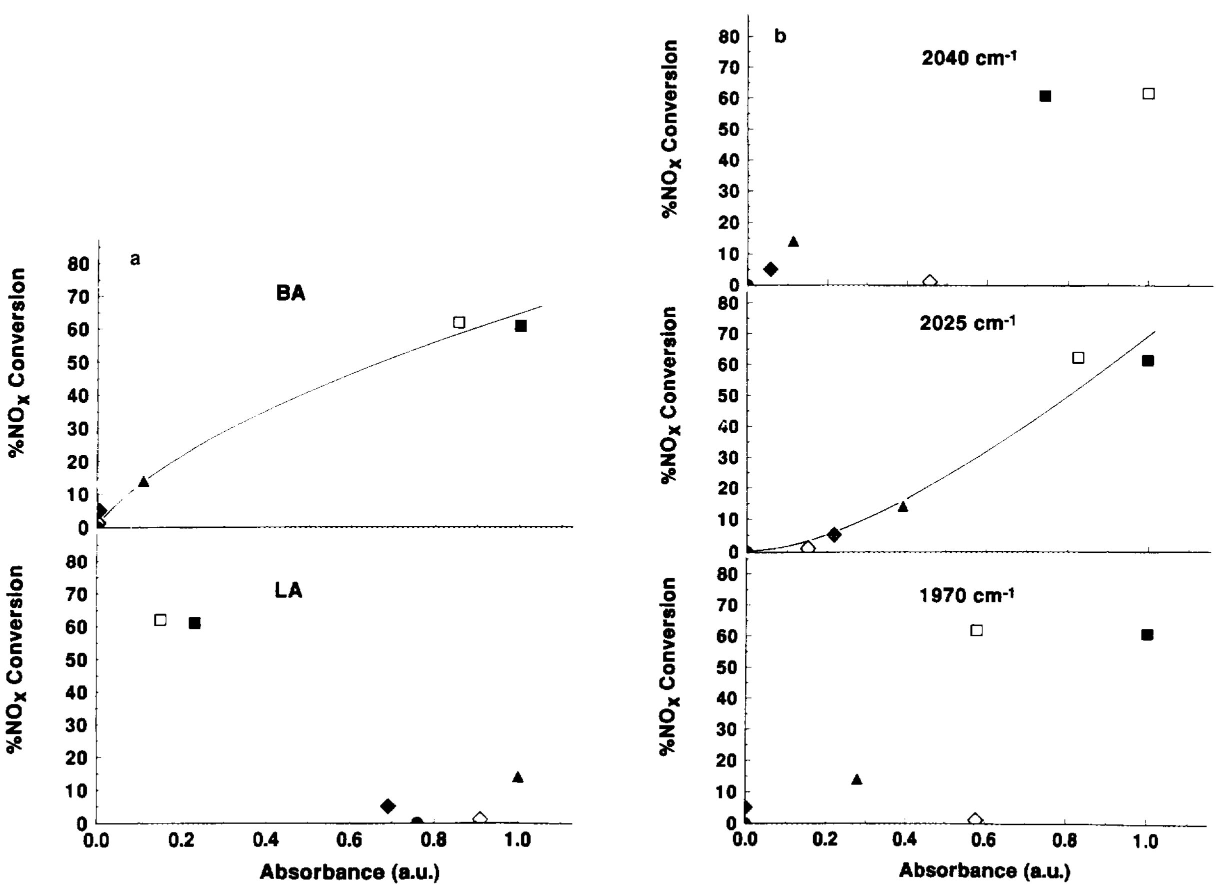

FIG. 4. Percent NOx conversion plotted as function of the absorbance of (a) the NH_4^+ band (BA) at around 1420 cm^{-1}, the coordinated NH_3 band (LA) at around 1605 cm^{-1}, and (b) the V=O overtone band at around 2040, 2025, and 1970 cm^{-1}. The symbols (◆), (▲), (■), and (●) designate 0.6, 2, and 6% V_2O_5/TiO_2 and TiO_2, respectively, under reaction in 500 ppm NO, 500 ppm NH_3, and 8% O_2. The symbols (□) and (◇) designate 6% V_2O_5/TiO_2 in similar reaction mixture but with 1 and 0% O_2, respectively.

sion of NO. Figure 4a shows the NO conversion plotted against the absorbances of NH_4^+ (on BA sites) and coordinated ammonia (on LA sites). Figure 4b shows NO conversion as a function of the absorbance of the three V=O band contributions at 2040, 2025, and 1970 cm^{-1}, where the absorbances of the first and last bands are estimated from differences between spectra in O_2 and in the reaction feed. Under fixed conditions, one observes a general increase in the NO conversion with the vanadia loadings (up to 6%). Figure 4 also shows the NO conversion measured with varying concentrations of O_2 (in 500 ppm NH_3, 500 ppm NO, at 525 K) on these samples. Reasonably good activity correlations are seen with the BA and the V=O overtone band at 2025 cm^{-1}, whereas an apparently inverse correlation is seen with LA sites. Thus, the results suggest that BA and V=O sites (the 2025 cm^{-1} band), and not the LA sites or the other V=O sites, may be involved in the catalytic cycle. Pure TiO_2 is almost inactive. It should be noted that the frequency for the NH_4^+ band is found to be lowest in the 6% vanadia/titania, indicating that the N–H bond is weakest in the 6% sample. Such changes were discussed in the preceding paper (19) and are in accordance with results in the literature (7, 23, 25, 27) on the structural changes in such catalysts. Thus, when comparing different catalysts, it is not only the number of BA sites which is expected to change but also the nature of the sites. Consequently, activity correlations are expected to be best when the process conditions and not the catalyst are changed.

In agreement with earlier adsorption studies (4, 19), no evidence for the presence of strongly adsorbed NO is detected in the present study for any of the samples during SCR reaction conditions. Thus, NO may be only weakly held on the surface and the SCR reaction apparently occurs between this weakly adsorbed NO species with more strongly adsorbed ammonia-type species.

Isotopic tracer experiments were carried out to study the interaction between NO and NH_3. When ^{15}NO was added to the 6% V_2O_5/TiO_2 with preadsorbed $^{14}NH_3$, a characteristic N_2O band was observed at 2178 cm^{-1} (rather than at 2224 cm^{-1} due to $^{14}N^{14}NO$ as usually seen with ^{14}NO and preadsorbed $^{14}NH_3$) reflecting the presence of $^{14}N^{15}NO$ (28). Furthermore, no bands could be detected at 2203 cm^{-1} and 2156 cm^{-1} due to $^{15}N^{14}NO$ and $^{15}N^{15}NO$, respectively.

Figure 5 compares the ammonia stretching regions of 6% V_2O_5/TiO_2 under SCR reaction condition at 525 K (Fig. 5a) with spectra measured in the mixture after the NO was removed (i.e., in flowing $NH_3 + O_2$) (Fig. 5b). The intensity of ammonia absorption bands is comparable in the two cases. The main difference lies in the greater intensity of the V–OH (3648 cm^{-1}) and NH_4^+ bands (between 2800–3020 cm^{-1}) during SCR reaction conditions (Fig. 5a). This difference is, as discussed above, attributed to new V–OH groups being formed under SCR reaction conditions. It should be noted that if NH_3 adsorption is carried out at the same temperature in the absence of oxygen (Fig. 5c), predominantly coordinated NH_3 (between 3100 and 3400 cm^{-1}) is observed. This behavior shows that in the absence of O_2, ammonia apparently converts the BA sites to LA sites at these temperatures, as also reflected by the negligible V–OH band intensity. Thus, under these conditions, it appears that ammonia reduces the catalyst and the Brønsted acid sites are therefore attributed to oxidized V–OH (V^{5+}–OH) species.

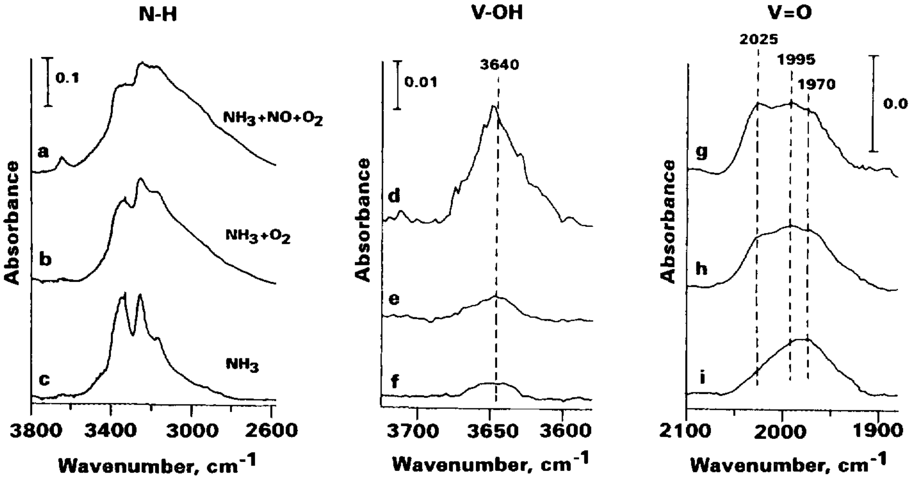

FIG. 5. *In situ* IR spectra of the N–H stretching region of the 6% V_2O_5/TiO_2 (a) under SCR reaction condition at 525 K, (b) in a flow of NH_3 + O_2/Ar at 525 K, and (c) in a flow of NH_3/Ar at 525 K, where (d)–(f) and (g)–(i) show the corresponding expanded V–OH and V=O overtone regions (gas phase NO subtracted), respectively.

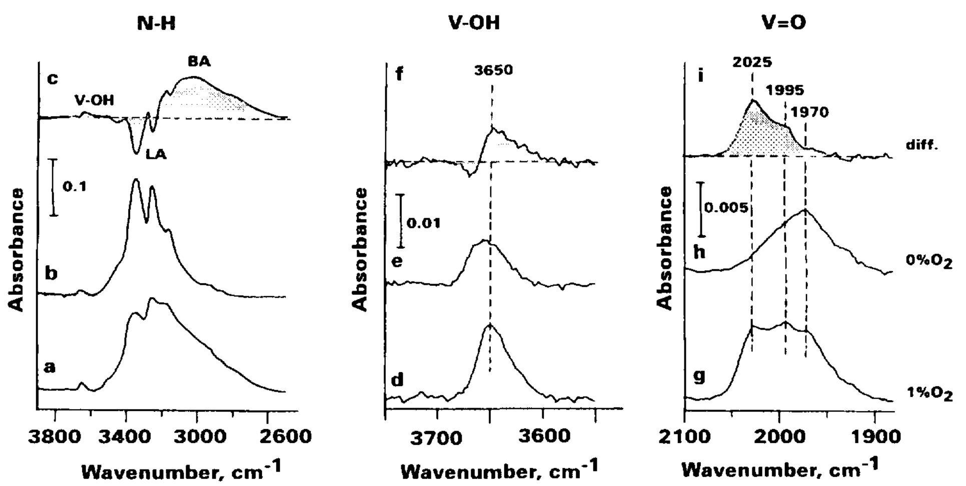

FIG. 6. *In situ* IR spectra of the 6% V_2O_5/TiO_2 in 500 ppm NH_3, 500 ppm NO, and (a) 1% O_2, (b) without O_2, at 525 K. Spectra (d), (e) and (g), (h) show the corresponding expanded V–OH and V=O overtone regions, respectively. The top spectra (c), (f), and (i) show the difference spectra in each region.

In view of the above results further experiments were conducted to understand the role of oxygen in the SCR reaction. *In situ* reaction studies were performed on the 6% vanadia/titania catalyst in the presence of different concentrations of oxygen. Decreasing the oxygen concentration from 8 to 1% resulted only in small decreases in activity and concentration of surface NH_4^+. However, significant differences were seen when the O_2 sample was completely removed. Figure 6 shows the spectra of the sample in the N–H, O–H stretching, and V=O overtone regions recorded in 500 ppm of NH_3, 500 ppm of NO, and 1% O_2 (bottom) and those recorded in the same gas mixture but in the absence of O_2 (middle). The changes caused by removal of O_2 are more clearly demonstrated in the difference spectra (top) (positive bands indicate the species which are removed upon removing O_2). The surface NH_4^+ concentration decreases upon removing O_2, as reflected by the positive band area in the high-frequency N–H stretching region (Fig. 6c), whereas the concentration of the coordinatively bonded NH_3 species increases. The difference spectrum in the V–OH region (Fig. 6f) shows a decrease of the OH band intensity and a shift upward upon removal of O_2. Concurrently, in the V=O overtone region (Fig. 6i), a clear decrease in the band at 2025 cm^{-1} is seen, whereas the band at 1970 cm^{-1} remains nearly constant. The simultaneous activity measurements show that the SCR reaction essentially stops when the O_2 is removed. These results show that BA sites and V=O species cannot be regenerated in the absence of O_2 to provide important sites for ammonia absorption and activation.

Figure 7 summarizes SCR activity and spectroscopic results for the V–OH region obtained during reaction in 500 ppm NH_3, 500 ppm NO, and 8% O_2 (Fig. 7b), 500 ppm NH_3, 500 ppm NO, and 1% O_2 (Fig. 7c), and after removing the oxygen for increasing lengths of time (Figs. 7d–7g). The changes in the V=O sites are shown in Figs. 7i–7n (corresponding to Figs. 7b–7g). The spectra of the oxidized sample in the same regions (Figs. 7a and 7h) are included for comparison. Nitric oxide conversions of 66% and 62% are measured in the presence of 8 and 1% oxygen, respectively. The NO conversion decreases to 58, 6, 2, and 1% after the O_2 is removed for 3, 30, 65, and

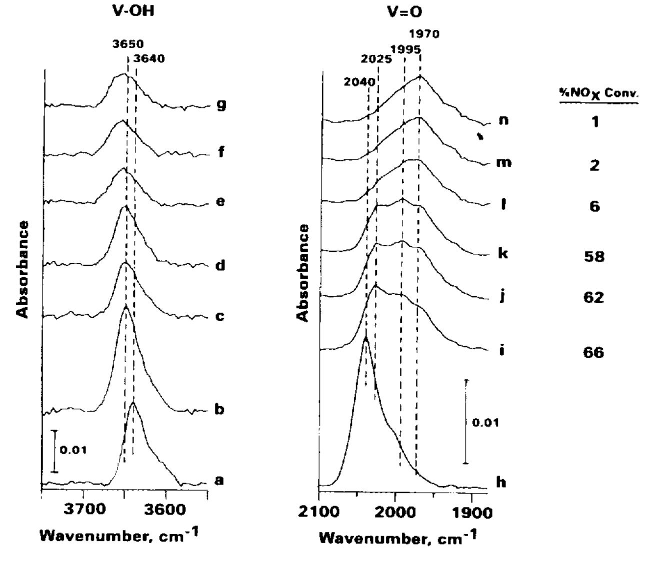

FIG. 7. *In situ* IR spectra of the 6% V_2O_5/TiO_2 during SCR reaction in 8% O_2 (b); during SCR reaction in 1% O_2 (c); after switching off O_2 for 3 min (d), 30 min (e), 65 min (f), and 90 min (g). The corresponding V=O overtone regions are shown in (i–n). Spectra (a) and (h) show the V–OH and V=O overtone band in the oxidized sample prior to reaction.

90 min, respectively. It is seen that the intensity of the V–OH band is highest in the SCR mixture with 8% O_2 and the position of this band does not change appreciably when the O_2 concentration is reduced to 1%. After O_2 has been switched off, however, the V–OH band is seen to shift progressively upward compared to the frequency observed in the presence of oxygen. A higher V–OH band frequency, as discussed above, suggests a more reduced state of V. Besides the band shift, the width of the band increases, reflecting a possible distribution of V–OH groups.

Under SCR reaction conditions in the presence of oxygen, three V=O bands at 2040, 2025, and 1995 cm^{-1} can be resolved in Figs. 7i and 7j, and these bands are due to terminal V=O groups with different environments. The intensity of the 2025 cm^{-1} band decreases as the concentration of O_2 decreases from 8 to 1%. Upon removal of O_2, this band is notably missing and only the band at 1970 cm^{-1} due to vanadyl species associated with reduced V species predominates on the surface. It appears from these results that the presence of the more oxidized terminal V=O groups at 2025 cm^{-1} is important for the SCR reaction. In the absence of oxygen, these species cannot be regenerated and are not present in appreciable amounts. Under these conditions, one observes the simultaneous presence of V–OH species associated with reduced V cations. The absence of the band at 2040 cm^{-1} under SCR reaction conditions suggests that the vanadyl species associated with this band are not regenerated at a sufficiently rapid rate in O_2 to be available for the SCR reaction.

The effects of changing the relative concentrations of NH_3 and NO have also been investigated and the results are summarized in Fig. 8. Figures 8a–8c show the IR spectra obtained during reaction at 575 K in gas feeds containing 8% O_2 with P_{NH_3}(ppm)/P_{NO}(ppm) ratios of 700/700, 700/100, and 100/700, respectively. It can be seen that at constant ammonia partial pressure the intensities of the ammonia absorption bands are not affected significantly by changing the NO partial pressure (Fig. 8a vs Fig. 8b). The fact that similar spectra were also observed in flowing $NH_3 + O_2$ also shows that NO does not adsorb significantly on the ammonia adsorption sites. Therefore, the ammonia coverage appears to be related only to the ammonia pressure under these SCR reaction conditions. In agreement with this result, the ammonia absorption bands essentially disappear when P_{NH_3} is reduced from 700 to 100 ppm, while keeping P_{NO} constant at 700 ppm. Thus, under the present range of conditions at constant O_2 concentration, the surface ammonia coverage is in equilibrium with the gaseous ammonia concentration. Traces of NO_2 begin to appear (centered at 1618 cm^{-1}) at higher NO pressures and as the ammonia is removed from the feed gas.

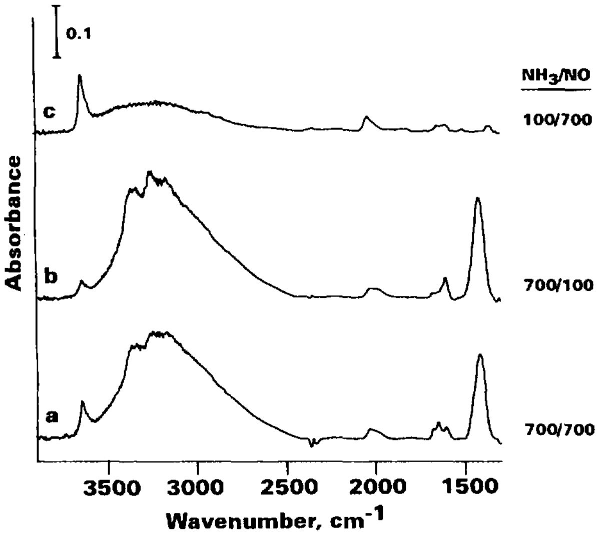

FIG. 8. *In situ* IR spectra of the 6% V_2O_5/TiO_2 obtained at 525 K during reaction in feed gas consisting of concentrations (in ppm) of NH_3 to NO of (a) 700/700, (b) 700/100, and (c) 100/700.

DISCUSSION

The present combined *in situ* FTIR and on-line mass spectrometric studies indicate that the overall catalytic cycle for the SCR reaction consists of the adsorption of ammonia on Brønsted acid sites, the reaction of some form of adsorbed ammonia with weakly adsorbed NO, and the regeneration of the active sites. We will now discuss the nature of each of these interactions and subsequently propose a catalytic cycle for the overall SCR reaction.

Adsorption of Ammonia

In agreement with earlier findings (4, 9, 10, 15, 19, 28), the *in situ* IR measurements reveal that ammonia is adsorbed on both Brønsted and Lewis acid sites under SCR reaction conditions, and adsorption appears to be stronger on the latter sites (7, 19). The present studies further show that NH_4^+ is the predominant species on high loading vanadia/titania catalysts under SCR reaction conditions. In previous papers (17, 19), Brønsted acidity has been shown to be related to V–OH groups. Several results in the present investigation show that the Brønsted acid sites are the active centers for the SCR reaction. For example, the concentration of Brønsted acid sites in catalysts with different loading is found to be correlated quite well with the NO conversion (Fig. 4a), whereas no positive correlation was seen with the Lewis acid sites. Furthermore, the experiments carried out in different O_2 concentrations at steady state (Fig. 7) or transient conditions (19) show a direct correlation of NO conversion with the concentration of Brønsted acid sites and an inverse correlation with the number of Lewis acid sites. The results obtained with different NH_3/NO ratios also agree with this conclusion.

We have also observed that the coverage of ammonia on the Brønsted acid sites during steady-state SCR reaction conditions is comparable to that observed during separate experiments in flowing $NH_3 + O_2$ at the same temperature. This behavior indicates that ammonia adsorption is fast and can be considered as an equilibrated step under typical SCR conditions. Thus, the SCR reaction is initiated by an adsorption equilibrium involving V^{5+}–OH sites:

$$NH_3 + V^{5+}\text{–OH} \Leftrightarrow V^{5+}\text{–ONH}_4. \quad [1]$$

Surface vanadyl groups also appear to play an important role in the SCR reaction. Ammonia adsorption leads to a downward frequency shift of these groups, reflecting a weakening of the V=O bond. This effect could indicate that reduction of V cations has occurred most probably via the transfer or partial transfer of H from ammonia to the surface. This behavior is also supported by the simultaneous formation of new OH species bonded to a more reduced V center upon reaction of ammonia with NO, as will be further discussed below. The vanadyl overtone band consists of more than one band reflecting the presence of several types of V=O in different environments (27). The present results suggest that it is mainly the monomeric terminal vanadyl species at 2025 cm^{-1} that are involved in this transformation of the adsorbed ammonia which may be expressed as

$$V^{5+}\text{–ONH}_4 + V^{5+}\text{=O} \Leftrightarrow V^{5+}\text{–ONH}_3\text{H}^+\text{–O–}V^{4+}. \quad [2]$$

We should note that the vanadyl species at 2040 cm^{-1} apparently does not participate in this reaction since its concentration is very low under reaction conditions. For example, this low concentration would suggest that the equilibrium of reaction [2] would lie far to the right, and the rate of the SCR reaction would be independent of the ammonia pressure. This behavior is not observed experimentally (18). Thus, it appears that the 2040 cm^{-1} vanadyl species is not regenerated sufficiently rapidly in O_2 to participate in the SCR reaction.

Previous kinetic analyses of the SCR reaction (18) suggested that adsorbed ammonia first must undergo an "activation step" before reaction with NO. No direct evidence for such a step was given. The present results have provided direct evidence for the existence for such a step, and it will be shown that the species produced in step [2] indeed reacts with NO.

Reaction of Activated Ammonia Complex with NO

Temperature programmed studies using FTIR to monitor the surfaces of vanadia/titania catalysts (19) have shown that NH_4^+ species react in flowing NO and NO + O_2, with simultaneous production of N_2 and H_2O accompanied by the formation of more reduced V–OH groups. The analysis of the V–OH groups produced by the SCR reaction showed that they consisted of both V^{5+}–OH and V^{4+}–OH. Similar studies in flowing oxygen did not show formation of new V^{4+}–OH groups, and most of the preadsorbed ammonia desorbed instead of reacting.

Although $^{14}N^{15}NO$ is not a major product at the temperatures studies here (29), the fact that trace amounts may be detected by IR when ^{15}NO is exposed to a vanadia/titania catalyst surface with preadsorbed $^{14}NH_3$ suggests that the SCR reaction occurs via interaction of NO with some form of adsorbed ammonia. Similar observations were made by others (30–32) using mixtures of ^{14}NO and $^{15}NH_3$. The fact that $^{15}N^{14}NO$ was not observed in the present study shows that the ^{15}NO bond initially does not dissociate and that NO attacks the nitrogen of surface ammonia species via the N atom of NO. This result also suggests that one of the N atoms of the N_2 product comes from NO, while the other atom is from NH_3.

Since significant amounts of strongly adsorbed NO have not been observed on the catalyst surface during transient experiments or under typical SCR reaction conditions, the reaction may be suitably described by an Eley–Rideal-type reaction between activated surface NH_4^+ species and gaseous or weakly adsorbed NO as proposed earlier (18). The above reaction may be described as

$$\begin{aligned} V^{5+}\text{–ONH}_3\text{H}^+\text{–O–}V^{4+} + NO &\Rightarrow N_2 + H_2O \\ &\quad + V^{5+}\text{–OH} + V^{4+}\text{–OH}^+. \end{aligned} \quad [3]$$

Regeneration of Active Sites

The present *in situ* on-line IR studies show that both V–OH and V=O species are involved in the SCR reaction. Ammonia adsorbs initially on V–OH and is subsequently activated on V=O. As mentioned above, reaction of the activated ammonia species with NO leads to SCR reaction products and new reduced V–OH sites. To regenerate the active sites, it is important to reoxidize these sites and, in fact, the SCR reaction stops in the absence of oxygen. The transient experiments (19) also showed that the oxidized V=O sites are most readily regenerated in the most oxidizing atmosphere, i.e., NO + O_2 > NO > O_2. This regeneration of V=O groups is accompanied by decreases in the V–OH band intensity and frequency to those values seen for initially oxidized samples (19). Thus, the results show that these oxidation treatments can return the catalyst surface to its originally oxidized state. In addition, the *in situ* on-line experiments with O_2 concentrations higher than about 1% show that the catalyst surface is predominantly in its oxidized state and exhibits high activity. Decreasing the oxygen concentration below this value results in a decrease in activity and an increase in reduced surface V–OH centers. At the same time, the V=O overtone region shows almost complete elimination of the terminal V^{5+}=O band near 2025 cm^{-1}, which is observed in high concentrations under conditions leading to high SCR reaction rates. These results show that in the absence of a significant concentration of O_2, the V^{5+}–OH and terminal V^{5+}=O groups needed for the ammonia adsorption and activation steps are not regenerated and the SCR reaction stops. The finding that TiO_2 may be capable of carrying out a stoichiometric SCR reaction (19) but not the SCR reaction in a catalytic manner suggests that equivalent redox sites are not present on pure titania and the active BA sites cannot be regenerated. These ideas suggest that the coexistence of a redox site, such as V=O, and a Brønsted acid site, such as V–OH, is required for the SCR reaction. The regeneration of the vanadyl species may be schematically considered to occur via the following types of steps:

$$2V^{4+}\text{–}OH^{+} \Rightarrow H_2O + V^{3+} + V^{5+}{=}O \qquad [4]$$

$$O_2 + 2V^{3+} \Rightarrow 2V^{5+}{=}O. \qquad [5]$$

Step [4] is probably not very fast, since reduced V^{4+}–OH species are observed under SCR reaction conditions. Since V^{3+} is not seen, step [5] is expected to be fast.

Formulation of Catalytic Cycle

The above results can be summarized schematically in Scheme 1, which shows a catalytic cycle for the SCR reaction under typical industrial conditions.

This scheme is composed of essentially two separate catalytic functions on the vanadia/titania catalyst, i.e., acid and redox functions. The SCR reaction is initiated by ammonia adsorption on Brønsted acid sites, or V^{5+}–OH. The adsorbed ammonia is then activated via the transfer or partial transfer of a H atom to the V^{5+}=O site, leading to some reduction of V. Gaseous or more likely weakly adsorbed NO subsequently reacts with this activated ammonia, yielding the reaction products, N_2 and H_2O, while releasing V^{5+}–OH and V^{4+}–OH (or some other more reduced vanadium hydroxyl than the V^{5+}–OH species). The cycle is then completed with the oxidation of V^{4+}–OH to V^{5+}=O.

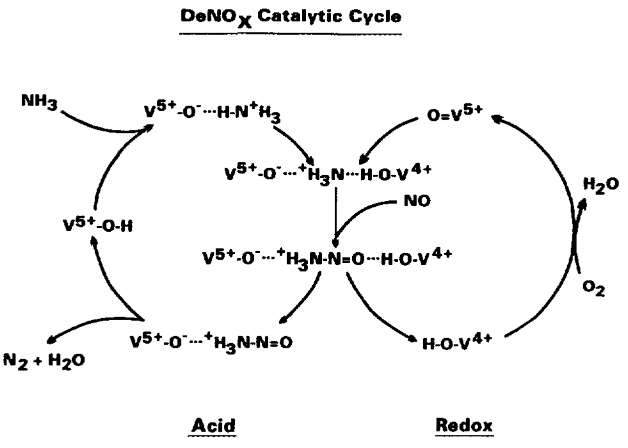

SCHEME 1. Proposed scheme illustrating the catalytic cycle of the SCR reaction over vanadia/titania catalyst.

The fact that the reduced or perturbed vanadyl and V–OH species may be observed under SCR conditions suggests that reoxidation of the catalyst is not very fast and may become an important step. Indeed, reducing the oxygen concentration from 8 to 1% (a value still in great excess of the value required by stoichiometry) is seen to increase the concentration of the reduced species and lower the rate of the SCR reaction.

Kinetic Implications of Catalytic Cycle

Previously, Dumesic *et al.* (18) have proposed the following reaction scheme to describe the NO conversion data as well as the ammonia slip behavior for vanadia/titania catalysts under industrial SCR conditions

$$NH_3 + M \Leftrightarrow NH_3\text{–}M \qquad \text{(fast)} \qquad [6]$$

$$NH_3\text{–}M + S \Leftrightarrow NH_3\text{–}S + M \qquad \text{(slow)} \qquad [7]$$

$$NO + NH_3\text{–}S \Rightarrow \text{Products} + S \qquad \text{(slow)}, \qquad [8]$$

where M represents an ammonia adsorption site and S represents a reactive site on which ammonia becomes activated. The activated ammonia subsequently reacts with NO in a slow step. The rate expression which follows from this mechanism is

$$r_{NO} = k_3 P_{NO} \frac{K_1 P_{NH_3}/P_{NO}}{1 + K_1 P_{NH_3}/P_{NO} + K_2/P_{NO} + K_{NH_3} P_{NH_3}}, \qquad [9]$$

where $K_1 = k_2 K_{NH_3}/k_3$ and $K_2 = k_{-2}/k_3$. Despite the success of this model, the identities of M and S sites were not well understood.

It is seen that the three steps [6]–[8] above are some of the steps in the catalytic cycle proposed in the present studies based on *in situ* FTIR and on-line activity measurements. Furthermore, the present results have provided further insight into the detailed nature of the different steps. For example, it is seen that the M sites in steps [6] and [7] are V^{5+}–OH, and the S sites in steps [7] and [8] can be identified as V^{5+}=O surface groups. Beside the three steps considered in the earlier study (18), we have

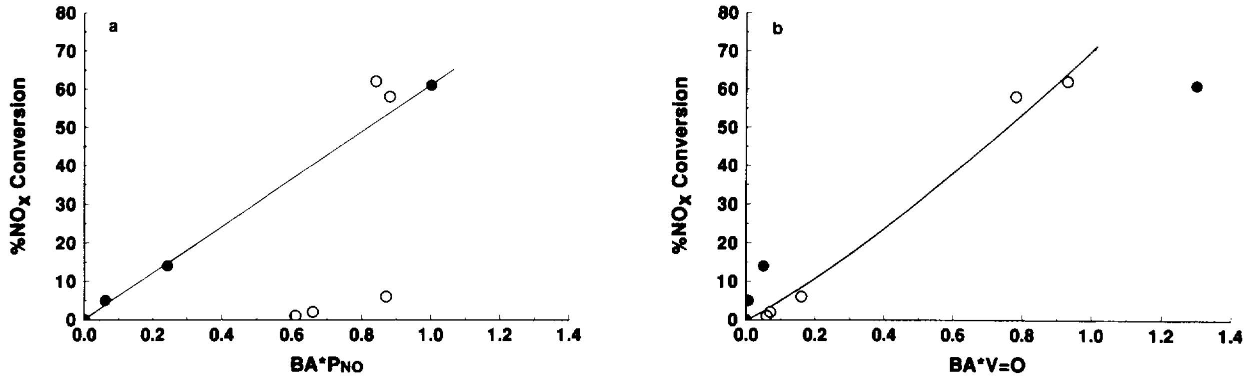

FIG. 9. Percent NO conversion plotted as functions of (a) BA · P_{NO} and (b) BA · V=O. (●) Data obtained at 8% O_2; (○) data obtained at ≤1% O_2).

also found evidence for additional surface redox reaction steps. The fact that reduced V–OH species (V^{4+}–OH) are observed during steady-state SCR conditions shows that catalyst reoxidation may also be important kinetically. Only quite small effects of O_2 were found when the O_2 concentration was reduced from 8 to 1%, but the effects are much more pronounced at lower oxygen concentrations. Effects of oxygen were also reported previously (3, 10, 33–37) and Went *et al.* (3) found significant effects on the SCR activity below 5000 ppm O_2.

The present study also shows that the type of activity correlation changes at high and low O_2 pressure. There is a rather good correlation (Fig. 9a) between the NO_x conversion and the product of the concentration of the Brønsted acid sites and the exit partial pressure of NO (BA · P_{NO}) for different catalysts during reaction with 500 ppm NO, 500 ppm NH_3, and 8% O_2. However, at oxygen concentrations lower than 1%, the correlation seen at higher O_2 concentration does not seem to apply. Instead, the activity appears to correlate with the product of the concentrations of the Brønsted acid sites and vanadyl groups (BA · V=O).

These results suggest that the relative importance of different steps changes depending on the oxygen concentration. At sufficiently high O_2 concentrations (8%), the ammonia activation step (step [2]) is fast and equilibrated, and the rate is equal to the rate of reaction of NO with activated ammonia (step [3]). Specifically, $r = k[\mathrm{BA}] \cdot [\mathrm{V{=}O}] \cdot P_{NO}$ or $r \propto k[\mathrm{BA}] \cdot P_{NO}$ since [V=O] is approximately constant. At low O_2 concentrations (1% or lower), the results indicate that step [2] becomes slow and irreversible since the rate of this step is $r = k[\mathrm{BA}] \cdot [\mathrm{V{=}O}]$.

Under most industrial SCR conditions, oxygen is usually present in large excess. Thus, in view of the above results we may expect that the rate is proportional to [BA] · P_{NO}. This then explains why a very good fit to industrial-type data could be obtained by considering only the three steps [6]–[8]. Under other conditions, the reoxidation steps ([4] and [5] in the cycle) may also become important and in order to explain data with large variations in oxygen partial pressure, a microkinetic model should include all the steps in the catalytic cycle.

CONCLUSIONS

Combined *in situ* FTIR and on-line activity measurements have been used to identify the nature of catalytic sites on vanadia/titania surfaces during actual SCR reactions. Brønsted acid sites, or the V–OH groups, are the important sites for ammonia adsorption on the vanadia/titania catalysts. One type of vanadyl groups are also found to be important in the catalytic cycle, since these species are responsible for activating the adsorbed ammonia. During this ammonia activation, the vanadyl groups are reduced and additional reduced V–OH are released upon subsequent reaction with NO. Finally, the reduced V–OH species are oxidized back to give the vanadyl groups, thereby completing the catalytic cycle. The rate expression derived from this catalytic cycle involving the cooperation of acid and redox sites can satisfactorily describe the SCR kinetics observed over a wide range of concentrations. The relative role of the different steps is seen to depend on the oxygen partial pressures with surface reoxidation becoming increasingly more important at low partial pressures. In environmental catalysis, one often has to deal with large changes in concentrations and it has previously been suggested that in such cases it may be especially dangerous to make simplified kinetic treatments (18, 38–40). The present results support that these shifts in the rate of the steps may take place and this necessitates a full microkinetic treatment. Whether other steps may play a role under other conditions is presently being examined.

ACKNOWLEDGMENTS

The authors thank T. Slabiak for supplying the sample, and K. Reiter and Y. Chen for technical assistance.

REFERENCES

1. Bosch, H., and Janssen, F., *Catal. Today* **2,** 369 (1988).
2. Odriozola, J. A., Heinemann, H., Somorjai, G. A., Garcia de la Banda, J. F., and Pereira, P., *J. Catal.* **119,** 71 (1989).
3. Went, G. T., Leu, L.-J., Rosin, R. R., and Bell, A. T., *J. Catal.* **134,** 492 (1992).
4. Topsøe, N.-Y., and Topsøe, H., *Catal. Today* **2,** 77 (1991).
5. Miyamoto, A., Yamazaki, Y., Hattori, T., Inomata, M., and Murakami, Y., *J. Catal.* **74,** 144 (1982).
6. Gasior, M., Haber, J., Machej, T., and Czeppe, T., *J. Mol. Catal.* **43,** 359 (1988).
7. Srnak, T. Z., Dumesic, J. A., Clausen, B. S., Törnqvist, E., and Topsøe, N.-Y., *J. Catal.* **135,** 246 (1992).
8. Takagi, M., Kawai, T., Soma, M. Onishi, T., and Tamaru, K., *J. Catal.* **57,** 528 (1979).
9. Takagi, M., Kawai, T., Soma, M., Onishi, T., and Tamaru, K., *J. Catal.* **50,** 441 (1977).
10. Inomata, M., Miyamoto, A., and Murakami, Y., *J. Catal.* **62,** 140 (1980).
11. Miyamoto, A., Kobayashi, K., Inomata, M., and Murakami, Y., *J. Phys. Chem.* **86,** 2945 (1982).
12. Bosch, H., Janssen, F. J. J. G., Oldenziel, J., van den Kerkhof, F. M. G., van Ommen, J. G., and Ross, J. R. H., *Appl. Catal.*, **25,** 239 (1986).
13. Janssen, F. J. J. G., van den Kerkhof, F. M. G., Bosch, H., and Ross, J. R. H., *J. Phys. Chem.* **91,** 5921 (1987).
14. Ramis, G., Busca, G., Lorenzelli, V., and Forzatti, P., *Appl. Catal.* **64,** 243 (1990).
15. Rajadhyaksha, R. A., and Knözinger, H., *Appl. Catal.* **51,** 81 (1989).
16. Chen, J. P., and Yang, R. T., *J. Catal.* **125,** 411 (1990).
17. Topsøe, N.-Y., *J. Catal.* **128,** 499 (1991).
18. Dumesic, J. A., Topsøe, N.-Y., Slabiak, T., Morsing, P., Clausen, B. S., Törnqvist, E., and Topsøe, H., *in* "Proceedings, 10th International Congress on Catalysis, Budapest, 1992" (L. Guczi, F. Solymosi, and P. Tétényi, Eds.), p. 1325. Akadémiai Kiadó, Budapest, 1993.
19. Topsøe, N.-Y., Topsøe, H., and Dumesic, J. A., *J. Catal.*, **151,** 226 (1995).
20. Topsøe, N.-Y., *Science* **265,** 1217 (1994).
21. Busca, G., Centi, G., Marchetti, L., and Trifiro, F., *Langmuir* **2,** 568 (1986).
22. Cristiani, C., Forzatti, P., and Busca, G., *J. Catal.* **116,** 586 (1989).
23. Busca, G., *Langmuir* **2,** 577 (1986).
24. Busca, G., *Mater. Chem. Phys.* **19,** 157 (1988).
25. Went, G. T., Oyama, S. T., and Bell, A. T., *J. Phys. Chem.* **94,** 4240 (1990).
26. Busca, G., and Lavalley, J. C., *Spectrochim. Acta, Part A* **42,** 443 (1986).
27. Went, G. T., Leu, L.-J., Lombardo, S. J., and Bell, A. T., *J. Phys. Chem.* **96,** 2235 (1992).
28. Little, L. H., *in* "Infrared Spectra of Adsorbed Species." Academic Press, New York, 1966.
29. Topsøe, N.-Y., Slabiak, T., Clausen, B. S., Srnak, T. Z., and Dumesic, J. A., *J. Catal.* **134,** 742 (1992).
30. Miyamoto, A., Kobayashi, K., Inomata, M., and Murakami, Y., *J. Phys. Chem.* **86,** 2945 (1982).
31. Vogt, E. T. C., Boot, A., van Dillen, A. J., Geus, J. W., Janssen, F. J. J. G., and van den Kerkhof, F. M. G., *J. Catal.* **114,** 313 (1988).
32. Vogt, E. T. C., van Dillen, A. J., Geus, J. W., Janssen, F. J. J. G., and van den Kerkhof, F. M. G., *J. Catal.* **119,** 270 (1988).
33. Svachula, J., Ferlazzo, N., Forzatti, P., Tronconi, E., and Bregani, F., *Ind. Eng. Chem. Res.* **32,** 1053 (1993).
34. Inameri, M., Watanabe, W., Matsuda, S., Nakajima, F., *in* "Proceedings, 7th International Congress on Catalysis, Tokyo, 1980" (T. Seiyama and K. Tanabe, Eds.), p. 841. Elsevier, Amsterdam, 1981.
35. Wong, W. C., and Nobe, K., *Ind. Eng. Chem. Prod. Res. Dev.* **25,** 179 (1986).
36. Bauerle, G. L., Wu, S. C., and Nobe, K., *Ind. Eng. Chem. Prod. Res. Dev.* **17,** 117 (1978).
37. Pearson, I. M., Ryu, H., Wong, W. C., and Nobe, K., *Ind. Eng. Chem. Prod. Res. Dev.* **22,** 381 (1983).
38. Dumesic, J. A., Rudd, D. F., Aparicio, L. M., Rekoske, J. E., and Trevino, A. A., *in* "The Microkinetics of Heterogeneous Catalysis." ACS, Washington, DC, 1993.
39. Rostrup-Nielsen, J. R., *in* "Elementary Reaction Steps in Heterogeneous Catalysis" (R. W. Joyner and R. A. van Santen, Eds.), p. 441. Kluwer, Netherlands, 1993.
40. Boudart, M., presented at ACS Spring Meeting, San Diego, 1994.